Engineering Science and Technology, an International Journal 21 (2018) 736–744

HOSTED BY

Contents lists available at ScienceDirect

Engineering Science and Technology, an International Journal

journal homepage: www.elsevier.com/locate/jestch

Full Length Article

Improved thermal management of computer microprocessors using cylindrical-coordinate micro-fin heat sink with artificial surface roughness

George Oguntala [a,*], Raed Abd-Alhameed [a], Gbeminiyi Sobamowo [b], Halimatu-Sadiyah Abdullahi [a]

[a] School of Electrical Engineering and Computer Science, Faculty of Engineering and Informatics, University of Bradford, West Yorkshire, UK
[b] Department of Mechanical Engineering, Faculty of Engineering, University of Lagos, Akoka, Lagos, Nigeria

ARTICLE INFO

Article history:
Received 27 December 2017
Revised 26 March 2018
Accepted 6 June 2018
Available online 19 June 2018

Keywords:
Improved electronic cooling
Micro-fin
Convective-radiative environment
Heat sink
Thermal management
Surface roughness

ABSTRACT

In this work, numerical study on the thermal behaviour and subsequent heat transfer enhancement of cylindrical micro-fin heat sink with artificial surface roughness is analyzed using Chebychev spectral collocation method. The developed thermal models consider variable thermal properties in accordance with linear, exponential and power laws. The numerical solutions are used to carry out parametric studies and to establish the thermal performance enhancement of the rough fins over the existing smooth fins. Following the results obtained from simulations, it is established that the thermal efficiency of the micro-fin is significantly affected by the geometric ratio, nonlinear thermal conductivity parameter, thermo-geometric parameter and the surface roughness of the micro-fin. In addition, the results show that geometric ratio and the surface roughness of the fin enhance its thermal performance. The fin efficiency ratio which is the ratio of the efficiency of the rough fin to the efficiency of the smooth fin is found to be greater than unity when the rough and the smooth fins are subjected to the same operations with the same geometrical, physical, thermal and material properties. From the investigation, it is established that improved thermal management of electronic and thermal systems can be achieved through the use of artificial rough surface fins or heat sink.

1. Introduction

The proliferation in demand for high-performance electronic systems often comes with inherent thermal challenges. With the thermal challenges for the present and next-generation electronics systems [1], the need to combate excess heat generation has been on the increase. Effective cooling technology or thermal management of microprocessors in most electronic devices including notebook and computers has been one of the key goals in modern-day advanced electronic design. To achieve this goal, active and passive modes of cooling technologies have been deployed. However, the active modes of heat transfer enhancement or augmentation such as fans, blowers, fluid vibration, surface vibration, suction and jet impingement and electrostatic fields have proved economically inviable due to their operating costs. An alternative means of thermal cooling is the applications of passive methods such as extended surfaces and treated surfaces, which have shown to be effective thermal management technology [2]. As one of the passive modes of thermal cooling technology, fin or extended surface are used to enhance the rate of heat transfer from thermal and electronic systems. Although there is a high record of thermal performance of extended surfaces in both electronic and thermal systems [3–16], the quest for more highly efficient, miniaturized, lightweight heat sink or fin with reduced thermal resistance continues. In search of such high-performance fin heat sink in their investigations, Zhou et al. [17] and Ventola et al. [2] advocated for the use of artificial surface roughness for transfer enhancement through extended surfaces. Consequently, different methods have proposed the application of artificial surface roughness in heat transfer surfaces [18–22]. However, experimental and theoretical investigations on thermal analysis of artificial rough surface micro-fins with application to microprocessors are limited. Nonetheless, Bahrami [23] presented a study on the effects of random rough surface on thermal performance of micro-fin. Diez et al. [24] applied the power series to analyze the thermal performance of rough micro-fins of three different profiles, namely, hyperbolic, trapezoidal and concave. Recently, several other authors carried out different numerical studies on the enhanced thermal

* Corresponding author.
E-mail address: g.a.oguntala@bradford.ac.uk (G. Oguntala).
Peer review under responsibility of Karabuk University.

https://doi.org/10.1016/j.jestch.2018.06.008
2215-0986/

Nomenclature

A_b	Cross-sectional area at the fin base, m^2
A_c	Cross-sectional area of the fin, m^2
$\overline{A}_c$	Average cross-sectional area of the rough fin, m^2
A_s	Surface area of the fin exposed to convection, m^2
$\overline{A}_s$	Average surface area of the rough fin exposed to convection, m^2
B_i	Biot number, given by $2r_bh/k$
k	Fin thermal conductivity, $Wm^{-1}K^{-1}$
L	Fin length, m^2
m	Thermo-geometric parameter, m^{-1}
m_σ	Mean absolute surface slope
M^2	Extended Biot number,
n	Heat transfer coefficient constant
P	Fin perimeter, m
q	Heat transfer rate,W
r	Fin radius, m
$\overline{r}$	Average radius of a rough fin, m
r_δ	Random variation of the fin radius in the angular direction, m
r_b	Radius at the fin base, m
r_L	Random variation of the fin radius in the longitudinal direction, m
r_t	Radius at the fin tip, m
T	Temperature, K
T_b	Base temperature, K
T_∞	Fluid temperature, K
M_c	Thermo-geometric ratio
x	Longitudinal coordinate, m
x_b	Position of base for the hyperbolic fin, m
x_t	Position of tip for the hyperbolic fin, m
z	Longitudinal coordinate, m

Greek symbols

$\mathscr{E}$	Relative roughness
φ	Dimensionless coordinate
η	Fin efficiency ratio
λ	Length of the arc of the fin profile, m
θ	Dimensionless temperature
σ	Isotropic surface roughness, m
σ_δ	Fin surface roughness in the angular direction, m
σ_L	Fin surface roughness in the longitudinal direction, m
ξ	Geometric ratio
ψ	Dimensionless coordinate

management of microprocessors heat sink using micro-fins with artificial surface roughness and variable thermal properties [24–29]. In most of these works, consideration is placed on the thermal performance in conductive-convective fins, with assumed constant thermal properties. However, such assumption becomes inaccurate with large temperature difference existing between the fin base and its tip. Therefore, this paper presents a numerical study on the thermal analysis and management of microprocessors using cylindrical rough pin micro-fin with variable thermal properties in a convective-radiative environment. The study is carried out to establish the influence of roughness, variable thermal performance, convective, radiative heat transfer on the thermal performance of the micro-fin. In addition, the developed thermal models are solved numerically using Chebychev spectral collocation method (CSCM) and simulated using ode45 in MATLAB.CSCM is an effective numerical approach that solves nonlinear integral and differential equations without linearization, discretization, closure, restrictive assumptions, perturbation, approximations, round-off error and discretization which often results in massive numerical computations. CSCM reduces the complexity of expansion of derivatives and the computational difficulties of the other traditional approximation analytical or perturbation methods. In addition, CSCM provides excellent approximations to the solution of non-linear equations with high accuracy, minimal calculation, and avoidance of physically unrealistic assumptions. It is not affected by computation round-off errors, whilst there is non-requisite for large computer memory and time. CSCM offers fast rate of convergence with a very large converging speed when compared with other numerical methods. The converging speed of the approximated numerical solution to the primitive problem is faster than one expressed by any power-index of *N-1*. The main advantage of CSCM lies in their accuracy for a given number of unknowns. For smooth problems in simple geometries, they offer exponential rates of convergence/spectral accuracy [30,31]. Thus CSCM is suitable for the present study for improved thermal management. Furthermore, this study is timely since most electronic/-computer devices require efficient, miniaturized cooling system. A key advantage of miniaturized heat sink with fan size is the reduction on the airflow rate and control of acoustic level, which results in lower distortion, an increases the lifespan on the electronic or computer component.The paper is organized as follows: In Section 2 we formulate the problem using cylindrical micro-fin with a rough surface. Section 3 presents the mathematical modeling of the rough surface, whilst in Section 4 we apply the CSCM to solve the developed thermal models in Section 3. Section 5 presents the fin efficiency. The results generated using MATLAB is presented and discussed in detailed in Section 6, whilst the paper concludes in Section 7.

2. Problem formulation

Consider a heat sink of a microprocessor is made up of rough cylindrical micro-fin shown in Fig. 1. Assume the fin is of dimension length L and thickness t, and exposed on both faces and subjected to a convective-radiative environment with temperature T_a, whilst no thermal contact resistance exists at the fin base. In addition, the micro-fin surface roughness is random and obeys a Gaussian probability distribution in the angular and longitudinal direction.For one-dimensional heat flow and following the assumptions stated above, the governing equations for the heat transfer in the fin can be summed as [32]:

$$\frac{d}{dx}\left(-k(T)A_c\frac{dT}{dx}\right)+h(T)P(T-T_\infty)=0 \tag{1}$$

The boundary conditions are given as:

$$x=0,\quad T=T_b x=L,\quad \frac{dT}{dx}=0 \tag{2}$$

The thermal conductivity of the micro-pin–fin can vary linearly as

$$k(T)=k_a(1+\lambda(T-T_\infty)) \tag{3a}$$

or exponentially as

$$k(T)=k_a e^{\lambda(T-T_\infty)}. \tag{3b}$$

The convective heat transfer coefficient will vary as

$$h(T)=h_b\left(\frac{T-T_\infty}{T_b-T_\infty}\right)^n. \tag{3c}$$

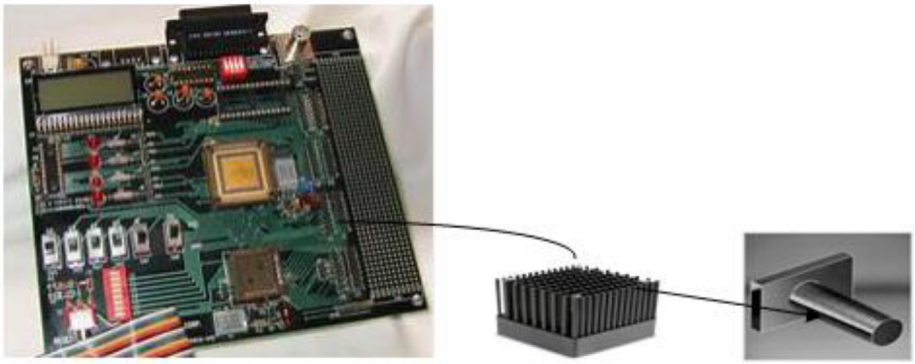

Fig. 1. (a) Motherboard of computer system with heat sink. Picture representation of (b) heat sink with cylindrical fins (c) cylindrical fin.

Table 1
Heat transfer modes constants.

Heat transfer mode	Multi-boiling heat transfer constant, n
Laminar film boiling or condensation	−1/4
Laminar natural convection	1/4
Turbulent natural convection	1/3
Nucleate boiling	2
Radiation	3
Constant heat transfer coefficient	0

Table 1 shows the various heat transfer modes with the constant n varying from −1/4 and 3. The constant n varies based on the mode of heat transfer as: (a) laminar film boiling or condensation (when $n = -1/4$), (b) laminar natural convection (when $n = 1/4$), (c) turbulent natural convection (when $n = 1/3$), (d) nucleate boiling (when $n = 2$), (e) radiation (when $n = 3$). However, when $n = 0$ it implies the heat transfer coefficient is constant.Substituting Eqs. (3a) and (3c), Eq. (1) becomes

$$k_a\frac{\partial A_c}{\partial x}\frac{\partial T}{\partial x}+k_aA_c\frac{\partial^2 T}{\partial x^2}+k_a\lambda(T-T_\infty)\frac{\partial A_c}{\partial x}\frac{\partial T}{\partial x}+k_a\lambda\overline{A_c}\left(\frac{\partial T}{\partial x}\right)^2 + k_a\lambda A_c(T-T_\infty)\frac{\partial^2 T}{\partial x^2}-\frac{h_bP(T-T_\infty)^{n+1}}{(T_b-T_\infty)^n}=0 \quad (4)$$

If the thermal conductivity varies exponentially according to the law $k(T)=k_ae^{\lambda(T-T_\infty)}$, we have

$$k_ae^{\lambda(T-T_\infty)}\frac{\partial A_c}{\partial x}\frac{\partial T}{\partial x}+k_a\lambda A_ce^{\lambda(T-T_\infty)}\left(\frac{\partial T}{\partial x}\right)^2+k_aA_ce^{\lambda(T-T_\infty)}\frac{\partial^2 T}{\partial x^2} -\frac{h_bP(T-T_\infty)^{n+1}}{(T_b-T_\infty)^n}=0 \quad (5)$$

3. Application of Chebyshev collocation spectral method

Assume the rough micro-fins have a random surface roughness that obeys the Gaussian probability distribution both in angular and longitudinal directions as shown in Figs. 2 and 3. Such an assumption is in line with the assumption in the previous works of Bahrami et al. [23] and Diez et al. [24].As shown from Figs. 2 and 3, it can be seen that the micro-fin artificial surface roughness is random, whilst the image in Fig. 2 show that the surface irregularities represents shallow variations of the surface height and slope. This, however, under such condition makes it difficult to obtain an exact value of the local radius for estimating the temperature of the rough micro-fin. Thus, probabilities for specific radii need to be managed, such that radius at every point (x, θ) of the micro-fin is defined as:

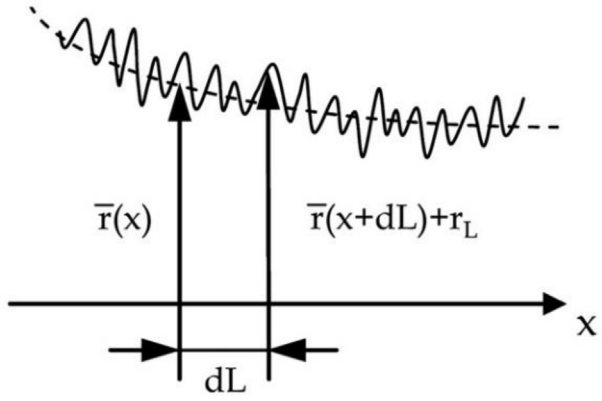

Fig. 2. Image of Cross-sectional view of generic pin fin of variable profile and rough surface [24].

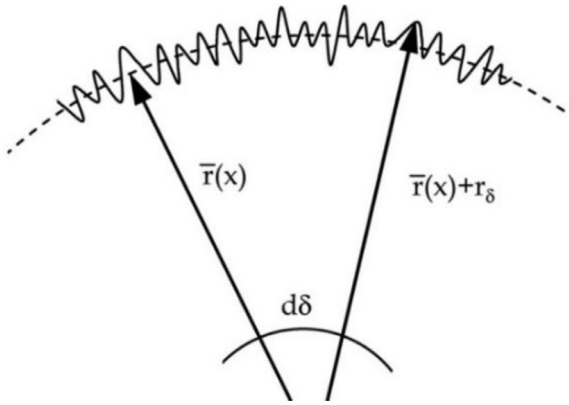

Fig. 3. Image of longitudinal-section of a generic pin fin of variable profile and rough surface as defined in [24].

$$r(x,\theta)=\bar{r}(x)+r_\delta+r_L \quad (6)$$

r_δ and r_L represents random variable radii along the angular and longitudinal directions, and around the mean radius $\bar{r}(x)$. Therefore, the Gaussian probability distribution function can be expressed as:

$$\Theta(r_\delta)=\frac{1}{\sqrt{2\pi\sigma_\delta}}e^{\left(-\frac{r_\delta^2}{2\sigma_\delta^2}\right)} \quad (7a)$$

$$\Theta(r_L) = \frac{1}{\sqrt{2\pi\sigma_L}} e^{\left(-\frac{r_L^2}{2\sigma_L^2}\right)} \tag{7b}$$

where σ_δ and σ_L are the standard deviations of the surface roughness of micro-fin in the angular and longitudinal direction. Thus, the average cross-sectional area A_c can, therefore, be estimated from the expression:

$$\overline{A_c}(x) = \pi\bar{r}(x)^2 \tag{8}$$

$$\text{where } \bar{r}(x)^2 = \int_{-\infty}^{\infty}\int_{-\infty}^{\infty}[\bar{r}(x) + r_\delta + r_L]^2\Theta(r_\delta)\Theta(r_L)\partial r_\delta \partial r_L \tag{9}$$

$$\text{Thus, } \bar{A}_c(x) = \int_{-\infty}^{\infty}\int_{-\infty}^{\infty}[\bar{r}(x) + r_\delta + r_L]^2\Theta(r_\delta)\Theta(r_L)\partial r_\delta \partial r_L \tag{10}$$

The integral limits range $-\infty to \infty$ is used since an unclipped Gaussian distribution is adopted. This is because unclipped Gaussian distribution gives more concentration density values for comparison for small/large variables with low probability. This, in effect, will result in accurate thermal prediction and subsequent enhancement for applied electronic and thermal systems. In addition, for change in variable to be carried out, $u_\delta = r_\delta/\sigma\}$ and $u_L = r_L/\sigma$, and the relative roughness ε specified using the radius at the fin base can be expressed as:

$$\varepsilon = \frac{\sigma}{r_b} \tag{11}$$

Therefore, Eq. (8) can be converted to:

$$\bar{A}_c(x) = \frac{1}{2}\int_{-\infty}^{\infty}\int_{-\infty}^{\infty}\left[\frac{\bar{r}(x)}{r_b\varepsilon} + u_\delta + u_L\right]^2 e^{-\left(\frac{u_\delta^2}{2}\right)} e^{-\left(\frac{u_L^2}{2}\right)}\sigma^2\partial u_\delta u_L \tag{12}$$

Since the average of u_δ and u_L is zero, then Eq. (12) reduces to:

$$\bar{A}_c(x) = \pi\bar{r}(x)^2 + 2\pi r_b^2\varepsilon^2 \tag{13}$$

On further simplification of Eq. (13), we have

$$\frac{\bar{A}_c(x)}{A_c(x)} = 1 + 2\left(\frac{\sigma}{\bar{r}(x)}\right)^2 \tag{14}$$

$$\frac{\partial\bar{A}_c}{\partial x} \approx \frac{\partial A_c}{\partial x} + 2\pi\bar{r}(x)m_\sigma = 2\pi\bar{r}(x)\sqrt{1+m_\sigma^2} \tag{15}$$

$$\bar{P}(x) = \frac{\partial\bar{A}_c}{dx} \approx 2\pi\bar{r}(x)\sqrt{1+m_\sigma^2} \tag{16}$$

where for a smooth perimeter, $P(x) = 2\pi\bar{r}(x)$

$$P(x) = P(x)\sqrt{1+m_\sigma^2} \tag{17}$$

and the mean absolute surface slope of the roughness component is given as,

$$m_\sigma = \frac{1}{L}\int_0^L\left|\frac{\partial(r-r_b)}{dx}\right|dx \tag{18}$$

On substituting Eq. (11) into Eq. (6), we have

$$\bar{A}_c(x) = \left(1 + 2\left(\frac{r_b}{\bar{r}(x)}\right)^2\mathscr{E}^2\right)A_c \tag{19}$$

On substituting Eqs. (1519) into Eq. (5), we derive the energy equation for the rough micro-fin as:

$$\begin{aligned}
&k_a\frac{\partial A_c}{\partial x}\frac{dT}{\partial x} + 2\pi\bar{r}m_\sigma\frac{\partial T}{\partial x} + A_c\frac{\partial^2 T}{\partial x^2} + 2\varepsilon^2 A_c\left(\frac{r_b}{\bar{r}}\right)^2\frac{\partial^2 T}{\partial x^2} + \lambda(T-T_\infty)\\
&\times\frac{\partial A_c}{\partial x}\frac{\partial T}{\partial x} + 2\pi\bar{r}m_\sigma\lambda(T-T_\infty)\frac{\partial T}{\partial x} + \lambda A_c\left(\frac{\partial T}{\partial x}\right)^2\\
&+ 2\varepsilon^2 A_c\lambda\left(\frac{r_b}{\bar{r}}\right)^2\left(\frac{\partial T}{\partial x}\right)^2 + A_c\lambda(T-T_\infty)\\
&\times\frac{\partial^2 T}{\partial x^2} + 2\varepsilon^2 A_c\lambda\left(\frac{r_b}{\bar{r}}\right)^2(T-T_\infty)\frac{\partial^2 T}{\partial x^2} - \frac{h_b P\sqrt{1+m_\sigma^2}}{k_a}\frac{(T-T_\infty)^{n+1}}{(T_b-T_\infty)^n} = 0
\end{aligned} \tag{20}$$

For cylindrical coordinate, A_c is constant, therefore $\frac{\partial A_c}{\partial x} = 0$where $\overline{r_c}(x) = r_b, P(x) = 2\pi r_b and \quad A_c(x) = \pi r_b^2$.Substituting these into Eq. (20), gives

$$\begin{aligned}
&\frac{\partial^2 T}{\partial x^2} + \frac{2m_\sigma}{r_b}\frac{\partial T_c}{\partial x} + \frac{2\lambda m_\sigma}{r_b}(T_c-T_\infty)\frac{\partial T_c}{\partial x} + \lambda\left(\frac{\partial T_c}{\partial x}\right)^2 + 2\varepsilon^2\frac{\partial^2 T_c}{\partial x^2}\\
&+ 2\varepsilon^2\lambda\left(\frac{\partial T_c}{\partial x}\right)^2 + \lambda(T_c-T_\infty)\frac{\partial^2 T_c}{\partial x^2} + 2\varepsilon^2\lambda\frac{\partial^2 T_c}{\partial x^2}\\
&- \frac{h_b P\sqrt{1+m_\sigma^2}}{r_b k_a}\frac{(T-T_\infty)^{n+1}}{(T_b-T_\infty)^n} = 0
\end{aligned} \tag{21}$$

Also, for the rough micro-fins with exponentially varying thermal conductivity, we have

$$\begin{aligned}
&(\lambda A_c e^{\lambda(T-T_\infty)}\left(\frac{\partial T}{\partial x}\right)^2 + 2\lambda\varepsilon^2 A_c e^{\lambda(T-T_\infty)}\left(\frac{r_b}{\bar{r}}\right)^2\left(\frac{\partial T}{\partial x}\right)^2 + e^{\lambda(T-T_\infty)}\frac{\partial A_c}{\partial x}\\
&\times\frac{\partial T}{\partial x} + 2\pi\bar{r}m_\sigma e^{\lambda(T-T_\infty)}\frac{\partial T}{\partial x} + A_c e^{\lambda(T-T_\infty)}\frac{\partial^2 T}{\partial x^2}\\
&+ 2A_c\varepsilon^2\left(\frac{r_b}{\bar{r}}\right)^2 e^{\lambda(T-T_\infty)}\frac{\partial^2 T}{\partial x^2} - \frac{h_b P\sqrt{1+m_\sigma^2}(T-T_\infty)^{n+1}}{k_a(T_b-T_\infty)^n} = 0)
\end{aligned} \tag{22}$$

For cylindrical coordinate, we arrived at

$$\begin{aligned}
&\lambda e^{\lambda(T_c-T_\infty)}\left(\frac{\partial T_c}{\partial x}\right)^2 + 2\lambda\varepsilon^2 e^{\lambda(T_c-T_\infty)}\left(\frac{\partial T_c}{\partial x}\right)^2 + \frac{2m_\sigma}{r_b}e^{\lambda(T_c-T_\infty)}\frac{\partial T_c}{\partial x}\\
&+ e^{\lambda(T_c-T_\infty)}\frac{\partial^2 T_c}{\partial x^2} + 2\varepsilon^2 e^{\lambda(T_c-T_\infty)}\frac{\partial^2 T_c}{\partial x^2}\\
&- \frac{2h_b\sqrt{1+m_\sigma^2}(T_c-T_\infty)^{n+1}}{k_a r_b(T_b-T_\infty)^n} = 0
\end{aligned} \tag{23}$$

Introducing the following dimensionless parameters into Eqs. (21) and (22),

$$\theta = \frac{T-T_a}{T-T_a}, X = \frac{x}{L}, \lambda(T-T_\infty) = \beta_\lambda, M_c^2 = \frac{h_b L^2}{k_a r_b}, \beta_c = \frac{x}{r_b}m_\sigma, \alpha_c = \mathscr{E}^2 \tag{24}$$

we arrived at the dimensionless governing equations as for the rough micro-fin with linearly varying and exponentially varying thermal conductivity, respectively as

$$\begin{aligned}
&\frac{d^2\theta_c}{dX^2} + \frac{2m_\sigma z_t}{r_b}\frac{d\theta_c}{dX} + \frac{2\beta_\lambda m_\sigma\theta_c z_t}{r_b}\frac{d\theta_c}{dX} + \beta_\lambda\left(\frac{d\theta_c}{dX}\right)^2 + 2\varepsilon^2\frac{d^2\theta_c}{dX^2}\\
&+ 2\varepsilon^2\beta_\lambda\left(\frac{d\theta_c}{dX}\right)^2 - \beta\theta_c\frac{d^2\theta_c}{dX^2} + 2\varepsilon^2\lambda\frac{d^2\theta_c}{dX^2} - 2M_c^2\sqrt{1+m_\sigma^2}\theta_c^{n+1}
\end{aligned} \tag{25}$$

and

$$\begin{aligned}
&\beta_\lambda e^{\beta_\lambda\theta_c}\left(\frac{d\theta_c}{dX}\right)^2 + 2\beta_\lambda\alpha_c e\beta_\lambda^{\lambda\theta_c}\left(\frac{d\theta_c}{dX}\right)^2 + 2\gamma_c e^{\beta_\lambda\theta_c}\frac{d\theta_c}{dX} + e\beta_\lambda^{\lambda\theta_c}\frac{d^2\theta_c}{dX^2}\\
&+ 2\alpha_c e^{\beta_\lambda\theta_c}\frac{d^2\theta_c}{dX^2} - 2X_c\theta_c^{n+1} = 0
\end{aligned} \tag{26}$$

If the fin is smooth and the thermal conductivity varies linearly, we have

$$\frac{d^2\theta_c}{d\psi^2}+\beta\theta\frac{d^2\theta_c}{d\psi^2}+\beta\left(\frac{d\theta_c}{d\psi}\right)^2-2M_c^2\theta^{n+1}=0 \tag{27}$$

For the smooth fin with exponentially varying thermal conductivity

$$e^{\beta\theta_c}\frac{d^2\theta_c}{d\psi^2}+\beta e^{\beta\theta_c}\left(\frac{d\theta_c}{d\psi}\right)^2-2M_c^2\theta^{n+1}=0 \tag{28}$$

The dimensionless boundary conditions are given as

$$\begin{aligned} &X=0, \quad \theta=1\\ &X=1, \quad \frac{d\theta}{dX}=0 \end{aligned} \tag{29}$$

In this work, the geometric ratio is given as $\xi=\frac{r}{L}$

4. Application of Chebyshev collocation spectral method

The development of exact analytical solutions for Eqs. (25)(28) is quite an undaunting task, if not almost impossible because of the presence of nonlinear terms in the equations. As a means of taking recourse to numerical methods, in this work Chebychev spectral collocation method (CSCM) is applied. As noted from our previous publication [30], Chebyshev collocation spectral method is accomplished starting with Chebyshev approximation for the approximate solution and generating approximations for the higher-order derivatives through successive differentiation of the approximate solution. Looking for an approximate solution, which is a global Chebyshev polynomial of degree N defined on the interval [-1, 1], the interval is discretized by using collocation points to define the Chebyshev nodes in $[-1,1]$, namely

$$x_j=cos\left(\frac{j\pi}{N}\right), \quad j=0,1,2,...N \tag{30}$$

The derivatives of the functions at the collocation points are given by:

$$f^n(x_j)=\sum_{j=0}^{N}d_{kj}^n f(x_j), \quad n=1,2. \tag{31}$$

where d_{kj}^n represents the differential matrix of order n and are given by

$$d_{kj}^1=\frac{4\gamma_j}{N}\sum_{n=0,l=0}^{N}\sum_{n+l=odd}^{n-1}\frac{n\gamma_n}{c_l}T_l^n(x_k)T_n(x_j), \quad k,j=0,1,...N, \tag{32}$$

$$d_{kj}^2=\frac{2\gamma_j}{N}\sum_{n=0,l=0}^{N}\sum_{n+l=even}^{n-1}\frac{n\gamma_n(n^2-l^2)}{c_l}T_l^n(x_k)T_n(x_j), \quad k,j=0,1,...N, \tag{33}$$

where $T_n(x_j)$ are the Chebyshev polynomial and coefficients γ_j and c_l are defined as:

$$\gamma_j=\begin{cases}\frac{1}{2} & j=0,\ or\ N\\ 1 & j=1,2,...N-1\end{cases} \tag{34a}$$

$$c_l=\begin{cases}2 & l=0,\ or\ N\\ 1 & l=1,2,...N-1\end{cases} \tag{34b}$$

As described above, the Chebyshev polynomials are defined on the finite interval $[-1,1]$. Therefore, to apply Chebyshev spectral method to our equation (11), we make a suitable linear transformation and transform the physical domain [-1, 1] to Chebyshev computational domain $[-1,1]$. We sample the unknown function w at the Chebyshev points to obtain the data vector $w=[w(x_o),w(x_1),w(x_2),\ldots w(x_N)]^T$. The next step is to find a Chebyshev polynomial P of degree N that interpolates the data $(i.e., \quad P(x_j)=w_j,\ j=0,1,\ldots N)$ and obtains the spectral derivative vector w by differentiating P and evaluating at the grid points $(i.e., \quad w_j'=P\prime(x_j)=w_j,\ j=0,1,\ldots N)$. This transforms the nonlinear differential equation into system nonlinear algebraic equations, which are solved by Newton's iterative method starting with an initial guess. Making a suitable transformation to map the physical domain [0,1] to a computational domain $[-1,1]$ to facilitate our computations.

$$\begin{aligned}&\frac{d^2\tilde{\theta}_c}{dX^2}+\frac{2m_\sigma z_t}{r_b}\frac{d\tilde{\theta}_c}{dX}+\frac{2\beta_\lambda m_\sigma\tilde{\theta}_c z_t}{r_b}\frac{d\tilde{\theta}_c}{dX}+\beta_\lambda\left(\frac{d\tilde{\theta}_c}{dX}\right)^2+2\varepsilon^2\frac{d^2\tilde{\theta}_c}{dX^2}\\&+2\varepsilon^2\beta_\lambda\left(\frac{d\tilde{\theta}_c}{dX}\right)^2-\beta\tilde{\theta}_c\frac{d^2\tilde{\theta}_c}{dX^2}+2\varepsilon^2\lambda\frac{d^2\tilde{\theta}_c}{dX^2}-2M_c^2\sqrt{1+m_\sigma^2}\tilde{\theta}_c^{n+1}\end{aligned} \tag{35}$$

and

$$\begin{aligned}&\beta_\lambda e^{\beta_\lambda\tilde{\theta}_c}\left(\frac{d\tilde{\theta}_c}{d\psi}\right)^2+2\beta_\lambda\alpha_c e\beta_\lambda^{\lambda\tilde{\theta}_c}\left(\frac{d\tilde{\theta}_c}{d\psi}\right)^2+2\gamma_c e^{\beta_\lambda\tilde{\theta}_c}\frac{d\tilde{\theta}_c}{d\psi}+e\beta_\lambda^{\lambda\tilde{\theta}_c}\frac{d^2\tilde{\theta}_c}{d\psi^2}\\&+2\alpha_c e^{\beta_\lambda\tilde{\theta}_c}\frac{d^2\tilde{\theta}_c}{d\psi^2}-2X_c\tilde{\theta}_c^{n+1}=0\end{aligned} \tag{36}$$

In the same way, the transformation for the smooth micro-fin was done.

The boundary conditions are

$$\tilde{\theta}(-1)=1, \quad \tilde{\theta}\prime(1)=0 \tag{37}$$

With the aid of CSCM on Eqs. (30) and (31), we arrived at a system of nonlinear algebraic equations, which could be expressed as

$$\begin{aligned}&\sum_{j=0}^{N}d_{jk}^2\tilde{\theta}_c(X_j)+\frac{2m_\sigma z_t}{r_b}\sum_{j=0}^{N}d_{jk}^1\tilde{\theta}_c(x_j)+\frac{2\beta_\lambda m_\sigma z_t}{r_b}\sum_{j=0}^{N}\tilde{\theta}_c(x_j)d_{jk}^2\tilde{\theta}_c(X_j)\\&+\beta_\lambda\left(\sum_{j=0}^{N}d_{jk}^1\tilde{\theta}_c(x_j)\right)^2+2\varepsilon^2\sum_{j=0}^{N}d_{jk}^2\tilde{\theta}_c(X_j)\\&+2\varepsilon^2\beta_\lambda\left(\sum_{j=0}^{N}d_{jk}^1\tilde{\theta}_c(x_j)\right)^2-\beta\sum_{j=0}^{N}\tilde{\theta}_c(x_j)d_{jk}^2\tilde{\theta}_c(X_j)\\&+2\varepsilon^2\lambda\sum_{j=0}^{N}d_{jk}^2\tilde{\theta}_c(X_j)-2M_c^2\sqrt{1+m_\sigma^2}\tilde{\theta}_c^{n+1}\end{aligned} \tag{38}$$

and

$$\begin{aligned}&\beta_\lambda\sum_{j=0}^{N}e^{\beta_\lambda\tilde{\theta}_c}d_{jk}^2\tilde{\theta}_c(X_j)\\&+2\beta_\lambda\alpha_c e^{\beta_\lambda\tilde{\theta}_c}\sum_{j=0}^{N}e^{\beta_\lambda\tilde{\theta}_c}d_{jk}^1\tilde{\theta}_c(X_j)\sum_{j=0}^{N}e^{\beta_\lambda\tilde{\theta}_c}d_{jk}^1\tilde{\theta}_c(X_j)\\&+2\gamma_c\sum_{j=0}^{N}e^{\beta_\lambda\tilde{\theta}_c}d_{jk}^1\tilde{\theta}_c(X_j)+\sum_{j=0}^{N}e^{\beta_\lambda\tilde{\theta}_c}d_{jk}^2\tilde{\theta}_c(X_j)\\&+2\alpha_c\sum_{j=0}^{N}e^{\beta_\lambda\tilde{\theta}_c}d_{jk}^2\tilde{\theta}_c(X_j)-2X_c\tilde{\theta}_c^{n+1}=0\end{aligned} \tag{39}$$

The boundary conditions are

$$\sum_{j=0}^{N}d_{kj}^1\tilde{\theta}(x_j)=0, \quad \tilde{\theta}(x_j)=1 \tag{40}$$

The above Eqs. (33) and (34) give systems of algebraic equations which are solved using Newton's iterative method.

5. Fin efficiency

The enhanced thermal performance of the micro-fin with the artificial surface could be established through the determination of fin efficiency as this is considered a key performance indicator in fin performance. In addition, following the definition from our previous publication [33], it could be deduced that the efficiency of the fin is expressed as:

$$\eta = \frac{Q_f}{Q_{\max}} = \frac{\int_0^L [Ph(T)(T - T_a)]\partial x}{Ph(T)L(T_b - T_a)} \tag{41}$$

Applying the dimensionless parameters, it can be shown that the dimensionless form of the efficiency is given as

$$\eta = \frac{Q_f}{Q_{\max}} = \int_0^L \theta_c^{n+1}(X)\partial X \tag{42}$$

The ratio of the efficiency of the rough fin to the smooth fin can be stated as

$$\frac{\eta_{rf}}{\eta_{sf}} = \frac{\int_0^L \theta_{rf}^{n+1}(X)\partial X}{\int_0^L \theta_{sf}^{n+1}(X)\partial X} \tag{43}$$

6. Result and discussion

The results of the numerical solutions for the temperature distribution of the rough fin, its rate of heat transfer and subsequent efficiency are plotted against dependent variables and other key variables of the model using MATLAB as shown in Fig. 4–11. From Figs. 4a and 4b., the effects of fouled Biot number on the temperature distribution of the fin are shown. From the figures, the presence of rough surface of the fin increases the temperature distribution and temperature uniformity in the fin.

Effects of thermal conductivity of the rough micro-fins on the temperature distribution are displayed in Figs. 5a and 5b when the thermo-geometric parameter is 0.5 and 1.0, respectively. It is indicated in the Figures that the increase nonlinear thermal conductivity parameter reduces the rate of heat transfer in the micro-fin as the temperature of the fin drops when the value of the nonlinear thermal conductivity parameter increases. This same trend is recorded for the study of the effects of the thermo-geometric parameter on the thermal performance of the fin as shown in Figs. 6 and 7. It should be noted that this result also represents the effects of increased thermal conductivity as depicted using different materials for improving the performance of the fin.

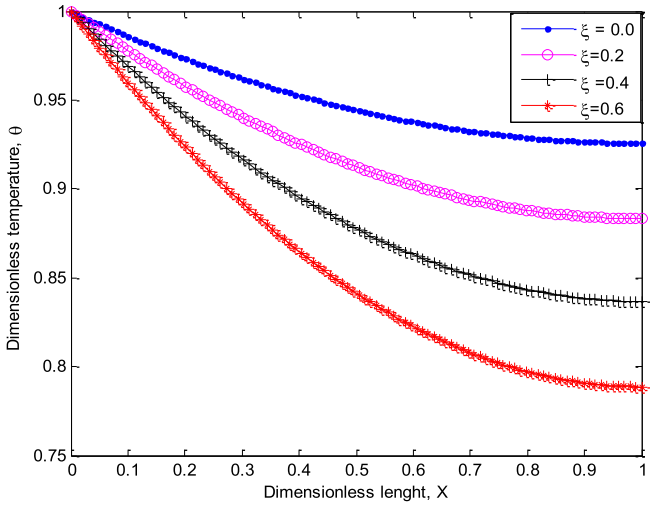

Fig. 4a. Effects of fouling Biot number on fin temperature when β = 0.3.

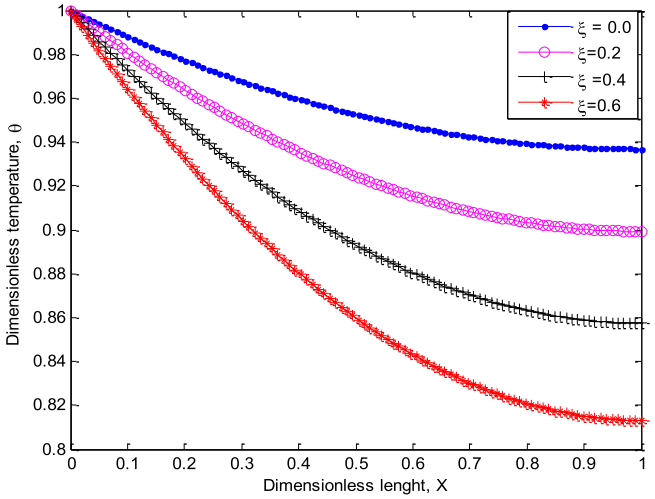

Fig. 4b. Effects of fouling Biot number on fin temperature when β = 1.0.

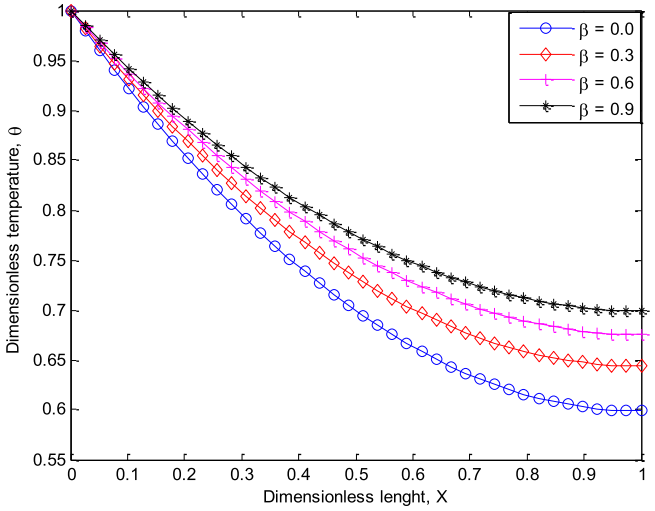

Fig. 5a. Effects of β on fin temperature when M_c = 0.5.

It is shown in Figs. 6 and 7 that the thermal efficiency of the micro-fin is significantly affected by the thermo-geometric ratio, nonlinear thermal conductivity parameter and the surface roughness of the micro-fin. From the figures, the fin efficiency decreases with increasing values of the thermo-geometric ratio M_c, whilst maintaining a low value of M_c improves the fin efficiency. This is because the artificial rough surface creates a thin or thick layer on the fin (depending on the thickness of the roughness) and the base of the rough fin. This layer increases the thermal resistance of the solid–fluid interface with the heat flow thereby resulting in a higher temperature at the surface of the fin. This implies that the thermo-geometric ratio and the surface roughness of the fin enhance its thermal performance.

Figs. 8 and 9 show the effects of thermal conductivity and artificial surface roughness on the fin efficiency ratio. The fin efficiency ratio which is the ratio of the efficiency of the rough fin to the efficiency of the smooth fin is shown in the figure to be greater than unity. This depicts an enhanced thermal performance in the rough

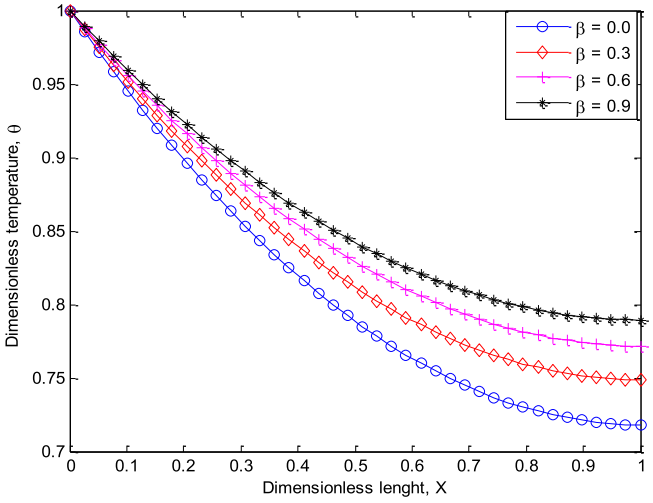

Fig. 5b. Effects of β on fin temperature when M_c = 1.0.

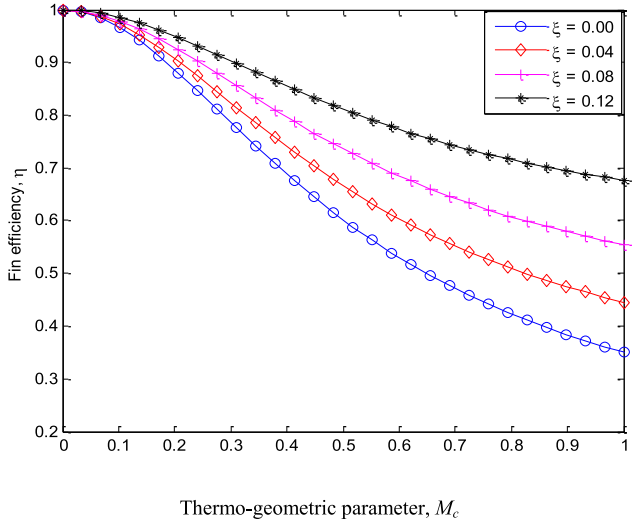

Fig. 6. Effects of geometrical ratio on fin efficiency.

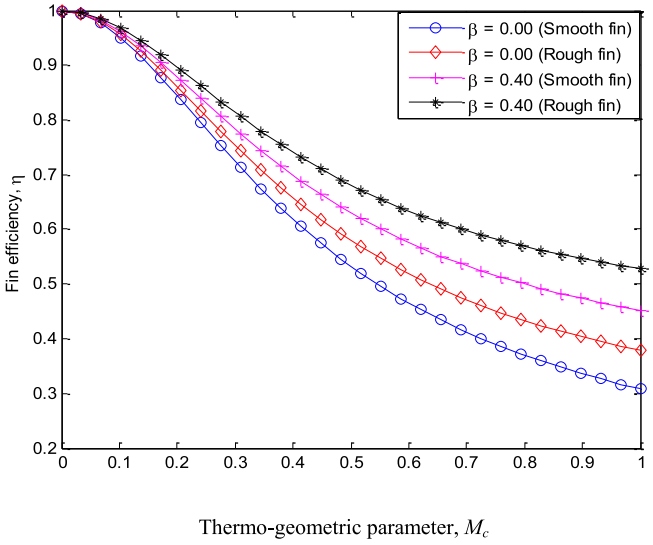

Fig. 7. Effects of thermal conductivity and surface roughness on the efficiency of the micro-fin.

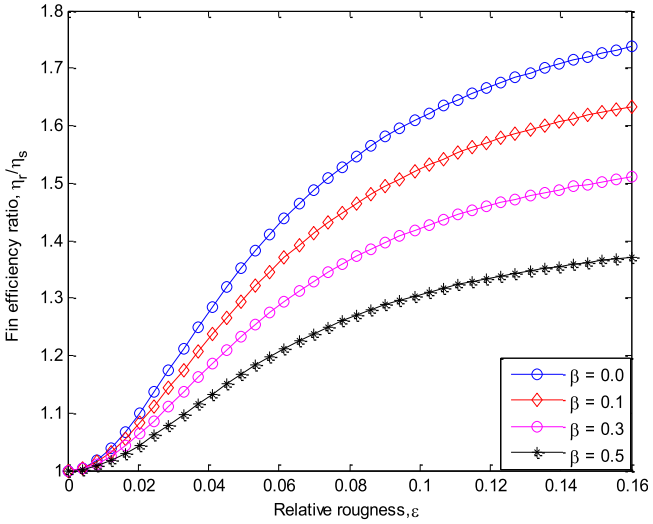

Fig. 8. Effects of thermal conductivity on fin efficiency ratio when M = 0.5.

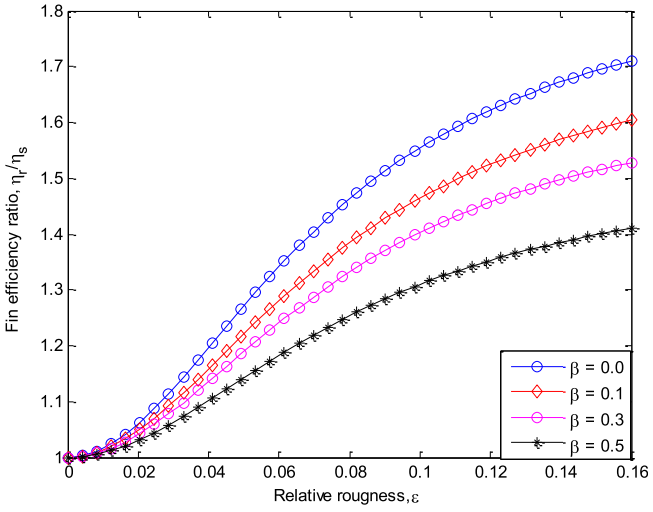

Fig. 9. Effects of thermal conductivity on fin efficiency ratio when M = 1.0.

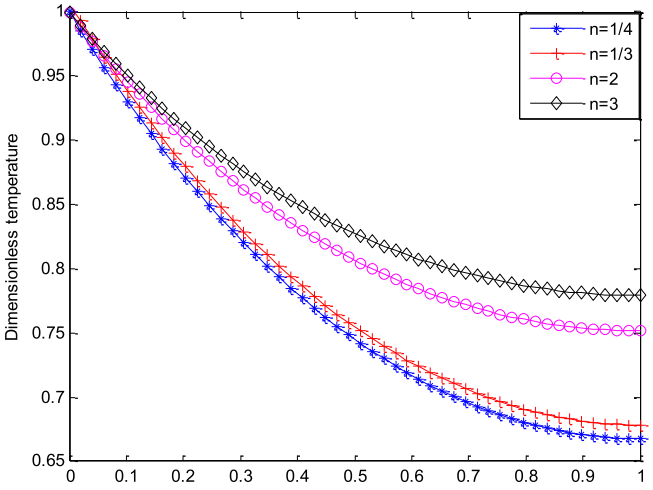

Fig. 10a. Dimensionless temperature distribution in the fin when M = 1.

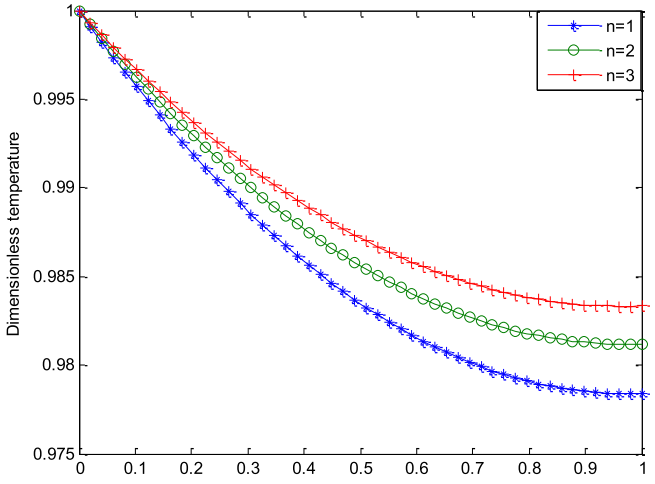

Fig. 10b. Dimensionless temperature distribution in the fin when M = 3.

Table 2
Comparison of established result with the present study.

η	NM	CSCM (present work)	Error
0.0	0.00000	0.00000	0.00000
0.1	0.15287	0.15288	0.00001
0.2	0.30155	0.30157	0.00002
0.3	0.44261	0.44262	0.00001
0.4	0.57320	0.57320	0.00001
0.5	0.69088	0.69087	0.00001
0.6	0.79337	0.79335	0.00002
0.7	0.87837	0.87836	0.00001
0.8	0.94330	0.94331	0.00001
0.9	0.98509	0.98508	0.00001
1.0	1.00000	1.00000	0.00000

fin as compared to the smooth fin. The surface rough roughness of the fin increases the thermal efficiency of the fin due to the increase in temperature uniformity in the rough fin and increased the temperature difference between the rough micro-fin and the bulk temperature.

Effects of multi-boiling constant on the temperature of the fin are shown in Figs. 10a and 10b. For the different values of the multi-boiling constant, it is depicted that the temperature distribution falls monotonically along the length of the extended surface. Also, the figures show that more heat is transferred to the environment through the fin at the lower values of the multi-boiling parameter than at its higher values.

Table 2 shows result comparison between the established results of NM using Runge-Kutta method coupled with shooting method and CSCM of the present study. The obtained results of efficiency using CSCM as compared with the numerical procedure indicates that both methods are in good agreements. The high accuracy of CSCM gives high confidence about the validity of the method in providing solution to the problem.

7. Conclusion

In this work, a numerical investigation on the thermal behaviour and subsequent heat transfer augmentation of cylindrical micro-fins with artificial surface roughness is studied using Chebychev spectral collocation method. The numerical solutions of the developed thermal models are used to carry out parametric study and to establish the thermal performance of the rough fin over the existing smooth fin. The results show that the geometric ratio and surface roughness of the micro-fin enhances its thermal performance. The study also establishes that the fin efficiency ratio is always greater than unity when the rough and the smooth fins are subjected to the same operational condition with the same geometrical, physical, thermal and material properties. The findings of this study are timely for the fabrication and miniaturization of heat sinks with rough surface area for electronic/computer systems. A key advantage of miniaturised heat sink with fan size is the reduction on the airflow rate and control of acoustic level, which results in lower distortion and subsequently increases the lifespan of any electronic or computer component.

References

[1] S.V. Garimella et al., Thermal challenges in next-generation electronic systems, IEEE Trans. Compon. Pack. Technol. 31 (4) (2008) 801–815.
[2] L. Ventola et al. Rough surfaces with enhanced heat transfer for electronics cooling by direct metal laser sintering Int. J. Heat Mass Trans. 2014 75 Supplement C 58 74
[3] P.M. Ligrani, M.M. Oliveira, T. Blaskovich, Comparison of heat transfer augmentation techniques, AIAA J. 41 (3) (2003) 337–362.
[4] X.L.M. Xiang Rui Meng, Ji Fu Lu, Xin Li Wei, A study on improving in natural convection heat transfer for heat sink of high power LEDs, advanced materials research Advanced Materials Research W. Fan Manufacturing Science and Technology, ICMST2011, 2011 6834–6839.
[5] C.J. Shih, G.C. Liu, Optimal design methodology of plate-fin heat sinks for electronic cooling using entropy generation strategy, IEEE Trans. Compon. Pack. Technol. 27 (3) (2004) 551–559.
[6] W.A. Khan, J.R. Culham, M.M. Yovanovich, The role of Fin geometry in heat sink performance, J. Electron. Pack. 128 (4) (2006) 324–330.
[7] Y.-T. Yang, H.-S. Peng, Numerical study of pin-fin heat sink with un-uniform fin height design, Int. J. Heat Mass Transf. 51 (19) (2008) 4788–4796.
[8] M. Wong et al., Convective heat transfer and pressure losses across novel heat sinks fabricated by Selective Laser Melting, Int. J. Heat Mass Transf. 52 (1) (2009) 281–288.
[9] E. Achenbach, The effect of surface roughness on the heat transfer from a circular cylinder to the cross flow of air, Int. J. Heat Mass Transf. 20 (4) (1977) 359–369.
[10] H. Honda, H. Takamastu, J.J. Wei, Enhanced boiling of FC-72 on silicon Chips with micro-pin-fins and submicron-scale roughness, J. Heat Transf. 124 (2) (2001) 383–390.
[11] E.K. Kalinin, G.A. Dreitser, Heat Transfer Enhancement in Heat Exchangers, Elsevier332, 1998, p. 159.
[12] F. Zhou, I. Catton, Numerical evaluation of flow and heat transfer in plate-pin fin heat sinks with various pin cross-sections, Numer. Heat Transf. Part A: Appl. 60 (2) (2011) 107–128.
[13] M.A. Elyyan, A. Rozati, D.K. Tafti, Investigation of dimpled fins for heat transfer enhancement in compact heat exchangers, Int. J. Heat Mass Transf. 51 (11) (2008) 2950–2966.
[14] J.R. Culham, Y.S. Muzychka, Optimization of plate fin heat sinks using entropy generation minimization, IEEE Trans. Compon. Pack. Technol. 24 (2) (2001) 159–165.
[15] C. Marques, K.W. Kelly, Fabrication and performance of a pin fin micro heat exchanger, J. Heat Transf. 126 (3) (2004) 434–444.
[16] L. Ventola et al., Micro-structured rough surfaces by laser etching for heat transfer enhancement on flush mounted heat sinks, J. Phys. Conf. Ser. 525 (1) (2014) 012017.
[17] F. Zhou, I. Catton, Obtaining closure for a plane fin heat sink with elliptic scale-roughened surfaces for Volume Averaging Theory (VAT) based modeling, Int. J. Therm. Sci. 71 (Supplement C) (2013) 264–273.
[18] W. Congshun, et al. Microfabrication of short pin fins on heat sink surfaces to augment heat transfer performance. in: 13th InterSociety Conference on Thermal and Thermomechanical Phenomena in Electronic Systems. 2012.
[19] N. Reimund et al., Additive manufacturing boosts efficiency of heat transfer components, Assemb. Automat. 31 (4) (2011) 344–347.
[20] A. Simchi, Direct laser sintering of metal powders: mechanism, kinetics and microstructural features, Mater. Sci. Eng. A 428 (1) (2006) 148–158.
[21] D. Manfredi et al., From powders to dense metal parts: characterization of a commercial AlSiMg alloy processed through direct metal laser sintering, Materials 6 (3) (2013) 856.
[22] F. Calignano et al., Influence of process parameters on surface roughness of aluminum parts produced by DMLS, Int. J. Adv. Manufact. Technol. 67 (9) (2013) 2743–2751.
[23] M. Bahrami, M.M. Yovanovich, R.J. Culham, Role of random roughness on thermal performance of microfins, J. Thermophys. Heat Transf. 21 (1) (2007) 153–157.
[24] L.I. Díez et al., Thermal analysis of rough micro-fins of variable cross-section by the power series method, Int. J. Therm. Sci. 49 (1) (2010) 23–35.
[25] H.-C. Chiu et al., The heat transfer characteristics of liquid cooling heat sink with micro pin fins, Int. Commun. Heat Mass Transf. 86 (2017) 174–180.
[26] J. Zhao et al., Numerical study and optimizing on micro square pin-fin heat sink for electronic cooling, Appl. Therm. Eng. 93 (2016) 1347–1359.

[27] L. Gong et al., Thermal performance of micro-channel heat sink with metallic porous/solid compound fin design, Appl. Therm. Eng. (2018).
[28] Y. Jia et al., Heat transfer and fluid flow characteristics of combined microchannel with cone-shaped micro pin fins, Int. Commun. Heat Mass Transf. 92 (2018) 78–89.
[29] L. Micheli, K.S. Reddy, T.K. Mallick, Experimental comparison of micro-scaled plate-fins and pin-fins under natural convection, Int. Commun. Heat Mass Transf. 75 (2016) 59–66.
[30] G. Oguntala, R. Abd-Alhameed, Thermal analysis of convective-radiative fin with temperature-dependent thermal conductivity using chebychev spectral collocation method, J. Appl. Computat. Mechan. 4 (2) (2018) 87–94.
[31] E.H. Doha, A.H. Bhrawy, S.S. Ezz-Eldien, Efficient Chebyshev spectral methods for solving multi-term fractional orders differential equations, Appl. Mathemat. Model. 35 (12) (2011) 5662–5672.
[32] G. Oguntala, R. Abd-Alhameed, G. Sobamowo, On the effect of magnetic field on thermal performance of convective-radiative fin with temperature-dependent thermal conductivity, Karbala Int. J. Modern Sci. (2017).
[33] G.A. Oguntala et al. Effects of particles deposition on thermal performance of a convective-radiative heat sink porous fin of an electronic component Therm. Sci. Eng. Progr. 2017